Dalton Transactions

PAPER

View Article Online
View Journal | View Issue

Cite this: *Dalton Trans.*, 2019, **48**, 628

Received 22nd October 2018,
Accepted 5th December 2018

DOI: 10.1039/c8dt04195d

rsc.li/dalton

Synthesis, characterization and catalytic epoxidation properties of a new tellurotungstate(IV)-supported rhenium carbonyl derivative†

Jingkun Lu, Xinyi Ma, Ping Wang, Junwei Feng, Pengtao Ma,
Jingyang Niu * and Jingping Wang *

A monomeric tellurotungstate(IV)-supported rhenium carbonyl derivative: $Na_2H_2[(CH_3)_4N]_6[Te_2W_{20}O_{70}\{Re(CO)_3\}_2]\cdot 20H_2O$ (**1**) has been successfully isolated and structurally characterized by single crystal X-ray diffraction crystallography, IR and UV-Vis spectroscopy, thermogravimetric analysis, *etc.* In particular, complex **1** could act as a efficient and reusable heterogeneous catalyst for selective epoxidation of various alkenes including different cycloalkenes, styrene derivatives, internal and long-chain alkenes. For example, *cis*-cyclooctene undergoes up to 98.2% conversion and >99% selectivity at 75 °C in acetonitrile with 30% H_2O_2 as an oxidant. Additionally, the electrocatalytic property of **1** for NO_2^- reduction was also investigated.

Introduction

The catalytic oxidation of alkenes has been a subject of growing interest in the production of fine chemicals and pharmaceuticals.[1] Epoxides are almost exclusively produced *via* the oxygenation of an alkene double bond. And they also constitute important intermediates for the production of fine and bulk chemicals, especially for the synthesis of natural products and synthetic analogues with biological activities.[2,3] Till know, various oxidants have been used in these catalytic system, such as iodosylarenes,[4] *m*-chloroperbenzoic acid,[5] organic peroxides and peracetic acid.[6,7] However, these oxidants above are all expensive and toxic, functioning with low atom economy and resulting in the generation of large amounts of waste.[8] Epoxidations that utilize hydrogen peroxide (H_2O_2) form only H_2O as a byproduct and, hence, do not require the regeneration or sale of organic co-products nor the remediation of environmentally impactful waste streams.[9] Therefore, from both economical and ecological viewpoints, the utilization of H_2O_2 as the oxygen donor is highly favored.

Notably, the Lewis acid character of the metal catalysts plays an important role in the activation of H_2O_2 and/or substrate for the catalytic oxygen-transfer reactions. Some notable electron-poor d^0 complexes of Ti^{IV}, Mo^{VI}, and W^{VI} have been applied for decades as homogeneous epoxidation catalysts.[10–12] Although tungsten-based catalysts display a highest activity for the epoxidation of alkenes,[13] very scare heterogeneous analogus with sufficient stability and activity are known.

The oxidation catalysis by polyoxometalates (POMs) has received much attention owing to their good catalytic features such as high activity and selectivity, controllable redox and acidic properties at the atomic or molecular level.[14] POMs are early transition-metal (M = Mo, W, V, Nb, Ta, *etc.*) oxygen cluster anions with discrete and versatile structures. In fact, POMs display a multitude of properties, and possible applications span a wide range of domains including catalysis, electrocatalysis, medicine, materials science, photochemistry *etc.*[15] As a peculiar branch of POMs, considerable attention has been directed toward POM-based metal carbonyl derivatives (PMCDs) because of their unique structures and potential catalytic properties in recent years.[16] For example, a isopentatungstate-supported metal carbonyl derivate $KH[(CH_3)_4N]_3\{[Re(CO)_3]_4[(\mu_2\text{-}OH)(\mu_3\text{-}O)(W_5O_{18})]\}\cdot 6H_2O$ reported by Niu *et al.* was found to be a highly efficient catalyst in the oxidation reaction of alkenes.[16i] However, PMCDs are still challenging like their radiation or thermal instability and dissolved incompatibility in most of the solvents *etc.* On the other hand, also tellurium can act as a heteroatom, but POMs containing tellurium are even less investigated. Between 1998 and 2003 Kreb's group reported the transition metal containing

---

Henan Key Laboratory of Polyoxometalate Chemistry, Institute of Molecular and Crystal Engineering, College of Chemistry and Chemical Engineering, Henan University, Kaifeng, Henan 475004, P. R. China. E-mail: jyniu@henu.edu.cn, jpwang@henu.edu.cn; Fax: (+86)371-23886876

† Electronic supplementary information (ESI) available: The bond valence sum calculations (Tables S1 and S2); selected bond lengths and angles (Table S3); additional structural figures (Fig. S1–S3); XPRD, IR, TG and UV-vis spectra (Fig. S4–S8); catalytic properties (Table S4, Fig. S9–S12). CCDC 1863573. For ESI and crystallographic data in CIF or other electronic format see DOI: 10.1039/c8dt04195d

derivates such as $[Mn_3(H_2O)_{10}(\beta\text{-}TeW_9O_{33})_2]^{8-}$, $[Co_3(H_2O)_8(WO_2)(\beta\text{-}TeW_9O_{33})_2]^{8-}$, $[(Zn(H_2O)_3)_2(WO_2)_2(\beta\text{-}TeW_9O_{33})_2]^{8-}$, $[Pd_3(\alpha\text{-}TeW_9O_{33})_2]^{10-}$.[17,18] In 2001, Kortz *et al.* reported the structure of $[Cu_3(H_2O)_3(\alpha\text{-}TeW_9O_{33})_2]^{10-}$.[19] In the following years, Korze's group reported preparation of various Te-containing lacunary polytungstates such as $[M_4(H_2O)_{10}(\beta\text{-}TeW_9O_{33})_2]^{4-}$ (M = Fe^{II}, Cr^{II}, Mn^{II}, Co^{II}, Ni^{II}, Cu^{II}, Zn^{II}, Cd^{II} and Hg^{II}), $[H_2Te_4W_{20}O_{80}]^{22-}$, $[TeW_9O_{33}]^{8-}$, $[Te_2W_{15}O_{54}]^{10-}$ and $[Te_3W_{21}O_{75}]^{12-}$.[20,21] Thus, tellurotungstate(IV)-supported metal carbonyl derivatives serving as potential heterogeneous catalysts grab our attention and provide an impetus for us to prepare such species. Up until now, only one example of tellurotungstate(IV)-supported rhenium carbonyl derivative $(NH_4)_3H_3[\{Mn(CO_3)\}(Mn(H_2O)_2)(Mn(H_2O)_3)(TeW_9O_{33})]_2\cdot 31H_2O$ was reported by our group in 2015.[22] In this paper, we report the X-ray crystallographic structure of a new Te(IV)-containing Krebs-type "slipped-sandwich" PMCD: $Na_2H_2[(CH_3)_4N]_6[Te_2W_{20}O_{70}\{Re(CO)_3\}_2]^{10-}$ (**1**). And the catalytic performance of **1** for the H_2O_2-based oxidation of various alkenes has been investigated under mild conditions.

Experimental

General methods and materials

All chemicals were commercially procured and used without any further purification. Elemental analysis for C, H and N was performed on a PerkinElmer 2400-II CHNS/O analyzer. Thermogravimetric analysis (TGA) was performed on a Mettler–Toledo TGA/SDTA 851^e instrument under nitrogen at a heating rate of 5 °C min^{-1} from 25–700 °C. The FT-IR spectra were recorded on a Bruker VEPTEX 70 IR spectrometer (using KBr pellets) in the range of 4000–500 cm^{-1}. X-ray powder diffraction (XPRD) spectral data were recorded on a Bruker AXS D8 Advance diffractometer with Cu Kα radiation in the angular range of 2θ = 5–45° at 293 K. UV-vis spectra were measured in a quartz cuvette with a path length of 1 cm by using a U-4100 spectrometer at room temperature. Electrochemical measurements were performed at room temperature with a CHI660 electrochemical workstation. A conventional three-electrode system was used. The working electrode was a freshly cleaned glassy carbon disk electrode, a platinum wire was used as the counter electrode and the saturated calomel reference electrode (SCE) was used as a reference electrode. GC-MS analyses were conducted using an Agilent 7890B gas chromatograph (with a 30 m × 0.32 mm × 0.25 μm/HP-5 ms quartz capillary column) equipped with a quadrupole mass-selective detector (Agilent MSD 5977). GC chromatogram was measured on Bruker 450-GC (FID) instrument, which was equipped with a 30 m column (GsBP-5, 0.25 μm film thickness and 0.25 mm internal diameter) with nitrogen as carrier gas.

Synthesis of $Na_2H_2[(CH_3)_4N]_6[Te_2W_{20}O_{70}\{Re(CO)_3\}_2]\cdot 20H_2O$ (1)

A sample of $Re(CO)_5Cl$ (0.0362 g, 0.1 mmol) was dissolved in 3 mL of CH_3CN, and then refluxed for 30 min at 70 °C (solution 1). $Na_2WO_4\cdot 2H_2O$ (0.56 g, 1.70 mmol) and Na_2TeO_3 (0.022 g, 0.099 mmol) were dissolved in 10 mL distilled water by using ultrasonic method. Then, the mixture was acidified further to pH 2.94 using 4 M HCl (solution 2). After that, solution 1 was added to the tellurium-containing solution 2, and the mixture was heated at 80 °C with stirring. After about 40 min, solid $(CH_3)_4NCl$ (0.1 g, 1.0 mmol) was added and the solution was stirred with a further 10 min, then cooled and filtrated. Slow evaporation at room temperature led to red crystals suitable for X-ray diffraction. Yield: 0.098 g (32.1%) for **1** based on $Re(CO)_5Cl$. Elemental analysis (%) calcd: C, 5.85; H, 1.56; N, 1.45. Found: C, 5.59; H, 1.81; N, 1.30. IR (KBr, cm^{-1}): 3437 (w), 2010 (vs), 1902 (vs), 1870 (vs), 1635 (w), 1485 (s), 967 (s), 862 (w), 818 (s), 773 (s), 741 (s), 692 (w), 656 (w), 514 (w), 482 (w).

Typical procedure for catalytic alkene epoxidations

Oxidation of various alkenes was carried out in a 50 ml round-bottom tube equipped with a reflux condenser. In a typical epoxidation reaction, a mixture of 1 mmol of alkenes, 5 mmol of catalyst, 5 mL of acetonitrile (MeCN) was added to the tube at the required temperature followed by the addition of 3 mmol of 30% H_2O_2. Then, the reaction mixture was stirred (800 rpm) for the requisite time at atmospheric pressure. At regular intervals, gas chromatography (GC) analysis was performed on an aliquot of reaction mixture using toluene as the internal standard. The recyclability of catalyst was also evaluated. After each run, the catalyst was simply filtered from the reaction mixture, washed thoroughly with acetonitrile, and dried at room temperature to be used in the next recycling experiment under identical reaction conditions.

X-ray crystallography

Suitable single crystal was selected from the mother liquors and airproofed in a glass tube. Intensity data for **1** was recorded on a Bruker APEX-II CCD diffractometer with the graphite-monochromated Mo Kα radiation (λ = 0.71073 Å) at 296 (2) K. The absorption correction was based on multiple and symmetry equivalent reflections in the data set using the SADABS program.[23] Using Olex2,[24] the structure was solved with the SHELXS-1997 structure solution program using Direct Methods and refined with the SHELXL refinement package using Least Squares minimisation.[25] In the final refinement, non-hydrogen atoms were refined anisotropically. Furthermore, a combination of elemental analysis and thermogravimetric analysis confirms the number of water molecules of crystallization in polyoxoanions. All H atoms on solvent water molecules were directly included into the final molecular formula. No hydrogen atoms associated with the water molecules were located from the difference Fourier map. A summary of the crystal data and structure refinements is listed in Table 1.

Results and discussion

Synthesis

Till now, the reports on new types of POM-based carbonyl metal derivatives are very rare mainly because most polyoxo-

Table 1 Crystal structure data for compound **1**

Formula	$C_{30}H_{114}N_6O_{96}Te_2W_{20}Re_2Na_2$
M_r (g mol^{-1})	6445.60
Crystal system	Monoclinic
Space group	$P2_1/n$
a (Å)	16.3974(9)
b (Å)	19.6444(11)
c (Å)	17.5409(10)
B (°)	93.0550(10)
V (Å^3)	5642.2(5)
Z	2
D_c (g cm^{-3})	3.609
μ (mm^{-1})	23.035
F (000)	5364.0
Crystal size (mm^3)	0.33 × 0.25 × 0.21
2θ range (°)	3.908 to 50.2
Reflections collected	28 704
Index ranges	$-19 \leq h \leq 17$, $-21 \leq k \leq 23$, $-20 \leq l \leq 12$
Data/restraints/parameters	10 033/111/642
GOF on F^2	1.126
R_1, wR_2 [$I > 2\sigma(I)$]	$R_1 = 0.0546$, w$R_2 = 0.1157$
R_1, wR_2 [all data]	$R_1 = 0.0771$, w$R_2 = 0.1251$

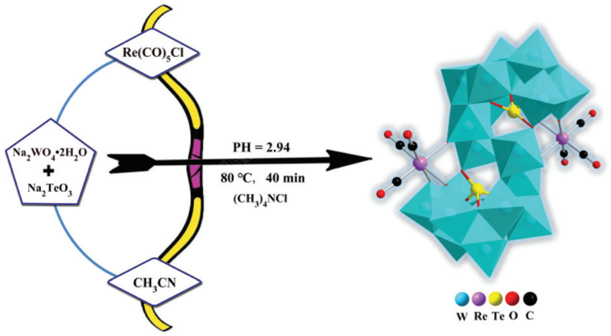

Scheme 1 The preparation process of **1**.

anions have not enough charge density to combine with carbonyl metal groups, along with their dissolved incompatibility, the radiation or thermal instability and the expensive prices of carbonyl metal compounds. In addition, a literature survey revealed very few reports on tellurium(IV)-containing polyoxotungstates, where the role of Te is largely limited to the primary hetero group. It is of great challenge for us to synthesize novel Te-containing PCMDs. Interestingly, several Krebs dimer complexes $[X_2W_{20}M_2O_{70}(H_2O)_6]^{(14-2n)-}$ (X = Sb, Bi; M = Fe, Co, Zn) are isolated by using the terminal aqua *fac*-$\{M(H_2O)_3\}^{2+/3+}$ groups replace the *fac*-$\{WO(OH)_2\}^{2+}$ moieties.[26] In light of this, considering the tricarbonyl *fac*-$\{M(CO)_3\}^+$ unit is also topologically equivalent to *fac*-$\{M(H_2O)_3\}^{2+/3+}$ and *fac*-$\{WO(OH)_2\}^{2+}$, four Krebs-type "slipped-sandwich" compounds $[XW_9O_{33}(WO_2)\{M(CO)_3\}]_2^{12-}$ (X = Sb, Bi and M = Re, Mn) were successfully obtained by Hill *et al.*[27] The preparation of the above complexes is conducted in a weakly acidic aqueous solution (pH 4.5–6.0), and these structures decomposed when pH value is lower than 3. However, in this paper, compound **1** was synthesized by a reaction of $Re(CO)_5Cl$, $Na_2WO_4·2H_2O$ and Na_2TeO_3 with a pH value of 2.94 at 80 °C, as presented in Scheme 1. Experimentally, using diluted HCl rather than HNO_3, H_2SO_4 and CH_3COOH solution to adjust pH value is especially important. Adjusting the pH to values higher than 3.3 or lower than 2.6, these reactions resulted solely in the formation of amorphous solid precipitates. Furthermore, the Na_2TeO_3 seem to play a key role in the successful formation of the cluster, and no crystals suitable for single-crystal X-ray diffraction could be obtained when Na_2TeO_3 was replaced by TeO_2 or $Te(NO_3)_4$.

Structural descriptions

Single-crystal X-ray diffraction analysis reveals that compound **1** crystallizes in the monoclinic space group $P2_1/n$ and consists of a discrete cluster anion $[Te_2W_{20}O_{70}\{Re(CO)_3\}_2]^{10-}$ (**1a**), Na/H/$[(CH_3)_4N]^+$ mixed cations, and lattice water molecules. Polyoxoanion **1a** is similar to that of the previously reported tricarbonyl metal polyoxoanion complexes $[X_2W_{20}O_{70}\{M(CO)_3\}_2]^{12-}$ (X = Sb, Bi and M = Re, Mn).[27] As shown in Fig. 1a, the crystal structure of **1** shows an idealized C_2 symmetry and comprises two $[TeW_{10}O_{35}\{Re(CO)_3\}]^{5-}$ fragments. Each carbonyl rhenium group *fac*-$\{Re(CO)_3\}^+$ is stabilized by a $[TeW_{10}O_{35}\{Re(CO)_3\}]^{5-}$ ligand in the "out-of-pocket" structural motif. Furthermore, two Re atoms and two central W atoms are located in the same plane (Fig. 1b). The fundamental common feature of the polyoxoanion is the trivacant {B-β-TeW_9O_{33}} Keggin fragments as the structural building unit. The {B-β-TeW_9O_{33}} units can be derived from the α-Keggin structure by removing one of the W_3O_{13} fragments. Additionally, the $[Te_2W_{20}O_{70}]^{12-}$ fragment can also be regarded as two identical {B-β-TeW_9O_{33}} units joined by two WO_6 octahedra (Fig. 1c). In polyoxoanion **1a**, all W atoms are six-co-

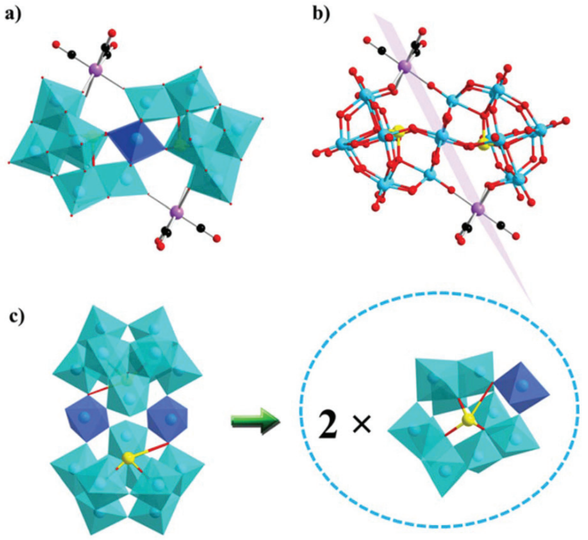

Fig. 1 Polyhedral and ball-and-stick representations of polyoxoanion **1a** (a and b). (c) Combined polyhedral/ball-and-stick representation of $\{Te_2W_{20}O_{70}\}$; two $\{TeW_{10}\}$ subunits. Color code: Te, yellow; W, blue; Re, purple; C, black; O, red; WO_6, cyan (two linkers are mazarine), all countercations and lattice water molecules are omitted for clarity.

ordinated with the usual octahedral geometry. The Re centers exhibit ReO_3C_3 coordination octahedra but with slight differences in relative bond distances [Re–C: 1.862–1.912 Å; Re–O: 2.144–2.163 Å]. And the Re–C bond distances is 1.883 Å on average, which is similar with that in analogous complexes reported previously.

Bond valence-sum (BVS) calculations show all W, Te atoms are in the +6 and +4 oxidation states, respectively (Table S1†). BVS results of all the oxygen atoms also indicate that the oxidation states are −2 (Table S2†).

IR, XRPD and TGA analyses

IR spectrum between 4000 and 450 cm^{-1} was used to investigate the structural characters of compound **1**. The signal appearing at 967 cm^{-1} can be ascribed to the characteristic absorption of $\nu(W{-}O_t)$. The characteristic peaks at 862–818 cm^{-1} and 773–656 cm^{-1} are derived from the $\nu(O_b{-}W{-}O_b)$ and $\nu(W{-}O_c)$ vibrations.[28] In addition, the strong absorption bands at 2010 cm^{-1} and 1902 cm^{-1} arise from symmetric and antisymmetric stretching vibration of the C–O bond, respectively.[29] Comparing with IR spectra of $Re(CO)_5Cl$ and compound **1** (Fig. S4–S5†), the peaks display obviously red shift, which may attribute to the combination of carbonyl metal groups with POM frameworks. The peak at 3037 cm^{-1} belongs to –OH and –NH stretching vibrations while the flexural vibrations of –OH and –NH are observed at 1635 and 1485 cm^{-1}, respectively, which shows the existence of water molecules and $(CH_3)_4N^+$. In addition, the resonance at 3437 cm^{-1} is attributed to water molecules. In addition, the purity of the phase has been checked by comparison of the experimental X-ray powder pattern with the powder pattern calculated from the structure solved from single-crystal X-ray diffraction data. On the other hand, the difference in the intensities of some diffraction peaks may be attributed to the preferred orientation of the crystalline powder sample (Fig. S6†).

Thermogravimetric analysis (TGA) was performed on **1** to determine its degree of hydration and thermal stability. The TGA curve of **1** can be viewed as two stages of weight loss, giving a total loss of 16.67% (calcd. 16.76%) in the temperature range of 25–700 °C. The first stage from 25–260 °C is ascribed to the loss of twenty lattice water molecules, and the observed weight loss 5.72% is consistent with the calculated value 5.78%. The second weight loss is 10.97% between 260–700 °C, which may be assigned to the removal of six CO (in the form of CO_2 molecules), six tetramethylammonium cations and two protons (in the form of constitutional water molecules) (calcd. 10.98%) (Fig. S7†).

CV spectra

In order to investigate the properties of **1** in the mixed solvent $CH_3CN{-}H_2O$ (1 : 3, volume ratio), the UV-vis spectra are monitored (Fig. S8†). Moreover, the UV-vis spectra of **1** in aqueous solution (5×10^{-5} mol L^{-1}) do not change over a period of 6 h at room temperature in a dark environment. Cyclic voltammetry (CV) experiments were performed to examine the electrochemical behaviors and electrocatalytic property of **1** in the mixed solvent $CH_3CN{-}Na_2SO_4$ (0.4 mol L^{-1}) (1 : 3, volume ratio). Three groups of waves appear in Fig. 2 (the top picture), one of them located in the positive and the others in the negative potential domain *versus* SCE. As expected, the W^{VI}-based waves are located at a more negative potential than that attributable to the Re^I center. In the negative potential, there exists two separated quasi-reversible redox couples of waves at $E_{1/2} = -0.601$ V (I/I′) and $E_{1/2} = -0.890$ V (II/II′) [$E_{1/2} = (E_{pc} + E_{pa})/2$]; E_{pc} and E_{pa} are the cathodic and anodic peak-potentials, respectively. The peaks I/I′ and II/II′ should be assigned to the two consecutive two-electron process of W centers. Moreover, the electron transfer of III/III′ is ascribed to the redox process of the $[Re(CO)_3]^+$ pendant. With the scan rates increasing, the cathodic peak potentials shift toward the negative direction and correspondingly the anodic peak potentials shift towards the positive direction, but the mean peak potential does not change distinctly. Below 200 mV s^{-1}, the peak currents of the five peaks were proportional to the scan rate, demonstrating that the redox process becomes diffusion-controlled, similar behaviours were observed in the case of the

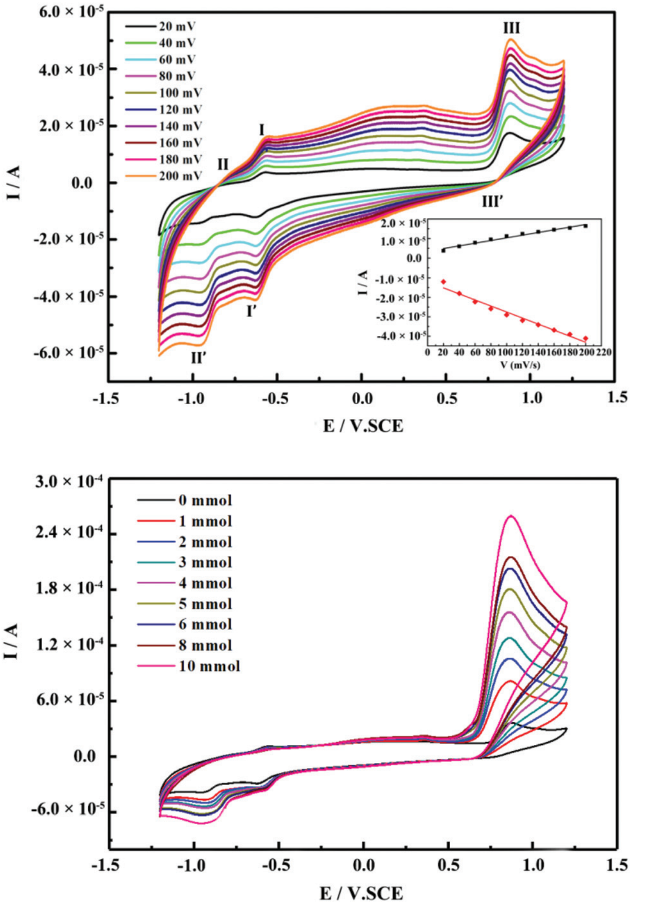

Fig. 2 CVs of **1** at different scan rates (top). Inset: Representation of the current as a function of the scan rate. CVs of **1** with different concentrations of $NaNO_2$: 0, 1.0, 2.0, 3.0, 4.0, 5.0, 6.0, 8.0, 10.0 mM, respectively, at a scan rate of 100 mV s^{-1} (bottom).

other compounds. In addition, previous studies have shown that POMs are capable of delivering the electrons to other species, thus serving as powerful electron reservoirs for multi-electron reductions and electro-catalytic processes. We found that **1** displays electrocatalytic activity to reduce nitrite (Fig. 2, the bottom picture). With the addition of modest amounts of sodium nitrite, all the reduction peak currents increase, and the corresponding oxidation peak currents decrease, thus demonstrating that both the two reduced species exhibit well electrocatalytic activity toward the reduction of nitrite. Obviously, as the concentration of nitrite continues to increase, the oxidation current of III/III′ starts to increase at a lower potential and further increases, indicating that compound **1** has high catalytic activity for nitrite oxidation. Also, the increase of oxidation peak III/III′ is more obvious than other two pairs of peaks, indicating that some intermediate products may be oxidized in the potential.

Catalytic oxidation

The epoxidation of alkenes is one of the most important reactions in the industrial chemistry because epoxides are key chemical intermediates. In this paper, reaction of *cis*-cyclooctene epoxidation with H_2O_2 as oxidant was selected as model to investigate the catalytic activity of complex **1** and other reaction parameters such as catalyst amount, reaction time and temperature (Table 2). Epoxidation reactions of *cis*-cyclooctene (1 mmol) were all conducted using H_2O_2 (3 mmol) in a solvent of acetonitrile. Blank reaction shows negligible *cis*-cyclooctene conversion in the absence of catalyst (entry 1). The 0.5 mmol% catalyst showed excellent catalytic activity with a conversion of 98.2% and selectivity of 99% at 75 °C within 0.5 h (entry 2). For the sake of comparison, the raw materials of $Re(CO)_5Cl$, $Na_2WO_4{\cdot}2H_2O$ and Na_2TeO_3 were all tested and almost inactive for the epoxidation (Table S4†). We found that a tellurium-containing heteropolymolybdate-supported rhenium carbonyl derivative reported by our group, $(NH_4)_8\{[Te_2Mo_{12}(OH)O_{44}][Re(CO)_3]\}{\cdot}13H_2O$,[30] was proved to be inefficient in the alkene epoxidation, indicating that W centers may be the catalytic active sites in the alkene epoxidation (Table S4†). The reaction was also carried out at three different temperatures under the same conditions by catalyst 1. The results shows that the conversions declined remarkably from 75 °C to 60 °C, indicating the vital impact on the reaction optimization process (entries 2–4). We can also find that the conversions increase with the reaction time prolonging (entries 2, 5–7). In addition, the effect of catalyst dosage is also a key factor in the reaction optimization process. In general, the higher the amount of catalyst applied, the higher are conversion. Reducing the catalyst loading to 0.1 mol% led to lower 45.8% conversion (entry 8). When slightly increasing the catalyst amount up to 0.3 mmol%, the reaction reaches 69.3% conversion (entry 9). Entries 2, 10 and 11 in Table 2 indicate the effect of oxidant amount on the catalytic performance. When the H_2O_2/substrate (O/S) molar ratio was varied from 1 : 1, 2 : 1 to 3 : 1, the degree of conversion of *cis*-cyclooctene ranged from 87.8, 92.5 to 98.2%, respectively. By facile separation, catalyst **1** can be directly reused in the subsequent experiments without any additional catalyst, yielding conversions of 98.0% and 96.8% for next two runs (Fig. 3). The XPRD patterns and IR spectra of the recovered catalysts showed the signature peaks corresponding to the original catalyst, indicating that framework structure of the catalyst was stable before and after the catalytic reaction (Fig. S10 and S11 in the ESI†).

Table 2 Effect of reaction parameters on model reaction of the alkene epoxidation catalyzed by **1** [a]

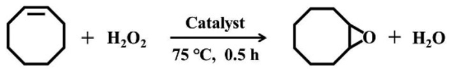

Entry	Catalyst (mol%)	T/°C	t/min	H_2O_2 [b]	Con. [c] (%)	Sel. (%)
1 [d]	—	75	30	3	2.9	>99%
2	0.5	75	30	3	98.2	>99%
3	0.5	60	30	3	32.4	>99%
4	0.5	65	30	3	42.4	>99%
5	0.5	75	5	3	38.4	>99%
6	0.5	75	15	3	79.6	>99%
7	0.5	75	20	3	86.9	>99%
8	0.1	75	30	3	45.8	>99%
9	0.3	75	30	3	69.3	>99%
10	0.5	75	30	1	87.8	>99%
11	0.5	75	30	2	92.5	>99%
12 [e]	0.5	75	30	3	98.0	98.1
13 [f]	0.5	75	30	3	96.8	97.6

[a] Reaction conditions: Substrate (1 mmol), catalyst **1**, and H_2O_2 were mixed in 5 mL acetonitrile. Unless otherwise noted. [b] H_2O_2/substrate ratio. [c] Determined by GC analyses using an internal standard technique based on methylbenzene. [d] Blank experiment. [e] Conversion and selectivity of the 2th cycle in the recycling studies. [f] Conversion and selectivity of the 3th cycle in the recycling studies.

Table 3 shows the results of oxidation of various kinds of organic substrates with 30% aqueous H_2O_2 catalyzed by **1**. In the presence of catalyst **1**, different terminal, internal, and cyclic alkenes were epoxidized high conversion. Obviously, the catalytic epoxidation of *cis*-cyclooctene affords the highest epoxide conversion (Table 3, entry 1). The epoxidation of cyclohexene proceeded efficiently and gave 1,2-epoxycyclohexane

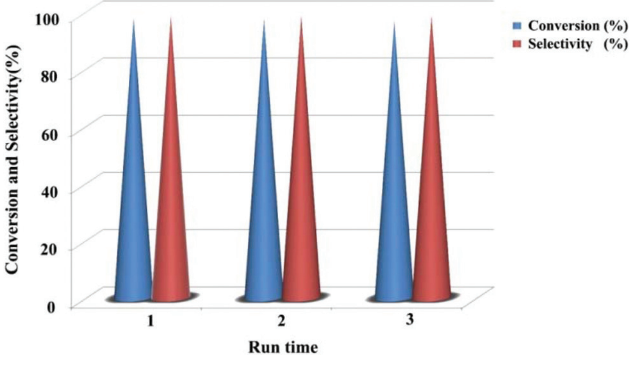

Fig. 3 Recyclability of the catalyst **1** for the epoxidation of cyclooctene. Reaction conditions: Catalyst (5 μmol); cyclooctene (1 mmol); H_2O_2 (3 mmol); MeCN (5 mL); reaction temperature (75 °C); time (0.5 h).

Table 3 Oxidation of various alkenes in water using H_2O_2 catalyzed by **1** [a]

Entry	Substrate	Time (h)	Product	Conv.[b] (%)	Sel. (%)
1		0.5	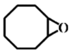	98.2	>99
2		5	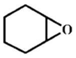	83.0	30.8
3	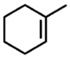	5	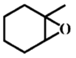	75.4	79.4
4	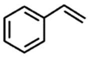	3	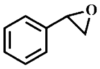	60.8	28.7
5	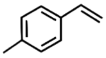	5	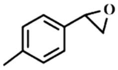	88.2	84.5
6	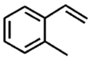	5	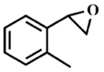	71.6	95.7
7	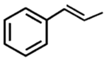	5	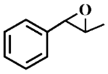	88.1	17.5
8	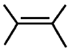	3	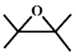	100	51.8
9		10	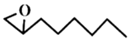	68.2	85.0
10[c]		5	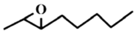	98.3	43.5

[a] Reaction conditions: Sulfides (1 mmol), catalyst (0.5 mol%), H_2O_2 (3 mmol); MeCN (5 mL), 75 °C. Unless otherwise noted. [b] Determined by GC analyses using an internal standard technique based on methylbenzene. [c] 50 °C.

quantitatively after 5 h (entry 2). 1-Methyl-cyclohexene as another cyclic alkene was epoxidized by this catalyst in 75.4% conversion and 79.4% selectivity (entry 3). Epoxidation of styrene proceeded to the corresponding epoxides with 60.8% conversion and 28.7% selectivity (entry 4). Furthermore, it was also found that the position property of the substituents of alkyl alkene should affect the conversions of corresponding products (entries 5 and 6). Compared with styrene, the difference mainly due to the electron-density and the steric hindrance at the C═C bond. In the epoxidation of α-methylstyrene, acetophenone was produced as minor products (entry 7). In addition, 2,3-dimethyl-2-butene, as an internal alkene, resulted in 100% conversion with 51.8% selectivity within 3 h (entry 8). In contrast, the reaction of terminal aliphatic alkene 1-octene showed moderate conversion of 68.2% to give 1,2-epoxyoctane after 10 h (entry 9). Catalyst **1** also catalysed the epoxidation of *trans*-2-octene, giving desired epoxide with a low 43.5% selectivity (entry 10). Linear alkenes took a longer time to yield epoxide products. This can be ascribed to the electron-deficient double bond that hinders the interaction between the alkene and active intermediates.[31] Additionally, the mainly side product of entries 2, 4, 7, 8 and 10 were 2-cyclohexen-1-one, ethanone, 1-phenyl-2-formyloxy, 1-phenyl-1,2-propanedione, (2,3,3-trimethyloxiranyl)methanol and 2,3-octanediol, respectively. And the mass spectra of the side products in the cases when epoxide selectivity was low were shown in Fig. S12.†

Conclusions

In summary, a new tellurotungstate(IV)-supported rhenium carbonyl derivative, $[Te_2W_{20}O_{70}\{Re(CO)_3\}_2]^{12-}$ was obtained by a conventional mixed-solvent solution method. The electrochemical experiments have shown that compound **1** exhibit good electrocatalytic activity for the reduction of NO_2^-. The catalytic performance of **1** in the epoxidation of different alkenes using H_2O_2 as an oxidant in acetonitrile was also demonstrated. Moreover, the catalyst was recovered easily and reused without significant loss in its catalytic activity. The preparation of **1** provides us with an effective and feasible way of designing novel tellurotungstate(IV)-supported rhenium carbonyl derivatives.

Conflicts of interest

There are no conflicts to declare.

Acknowledgements

We are grateful to the financial support from the National Science Foundation of China (20771034, 21401042), and the National Key R&D Program of China (2018YFB0605802).

Notes and references

1 (*a*) D. Banerjee, R. V. Jagadeesh, K. Junge, M.-M. Pohl, J. Radnik, A. Brückner and M. Beller, *Angew. Chem., Int. Ed.*, 2014, **53**, 4359; (*b*) W. J. Choi and C. Y. Choi, *Biotechnol. Bioprocess Eng.*, 2005, **10**, 167; (*c*) A. Fingerhut, O. V. Serdyuk and S. B. Tsogoeva, *Green Chem.*, 2015, **17**, 2042; (*d*) S. Bhattacharjee, D.-A. Yang and W.-S. Ahn, *Chem. Commun.*, 2011, **47**, 3637; (*e*) A. S. Novikov, M. L. Kuznetsov, B. G. M. Rocha, A. J. L. Pombeiro and G. B. Shul'pin, *Catal. Sci. Technol.*, 2016, **6**, 1343.

2 W. J. Choi and C. Y. Choi, *Biotechnol. Bioprocess Eng.*, 2005, **10**, 167.

3 (*a*) C. Wang and H. Yamamoto, *J. Am. Chem. Soc.*, 2014, **136**, 1222; (*b*) Q.-H. Xia, H.-Q. Ge, C.-P. Ye, Z.-M. Liu and K.-X. Su, *Chem. Rev.*, 2005, **105**, 1603; (*c*) B. Qi, X.-H. Lu, S.-Y. Fang, J. Lei, Y.-L. Dong, D. Zhou and Q.-H. Xia, *Mol. Catal.*, 2011, **334**, 44; (*d*) B. S. Lane and K. Burgess, *Chem. Rev.*, 2003, **103**, 2457; (*e*) P.-Z. Li, X.-J. Wang, J. Liu, J. S. Lim, R. Zou and Y. Zhao, *J. Am. Chem. Soc.*, 2016, **138**, 2142; (*f*) O. A. Wong and Y. Shi, *Chem. Rev.*, 2008, **108**, 3958.

4 (*a*) K. Nehru, S. J. Kim, I. Y. Kim, M. S. Seo, Y. Kim, S.-J. Kim, J. Kim and W. Nam, *Chem. Commun.*, 2007, 4623; (*b*) J. P. Collman, L. Zeng and J. I. Brauman, *Inorg. Chem.*, 2004, **43**, 2672; (*c*) L. A. Berben and J. C. Peters, *Inorg. Chem.*, 2008, **47**, 11669; (*d*) C. Fraser, L. Johnston, A. L. Rheingold, B. S. Haggerty, G. K. Williams, J. Whelan and B. Bosnich, *Inorg. Chem.*, 1992, **31**, 1835.

5 (*a*) S. H. Lee, L. Xu, B. K. Park, Y. V. Mironov, S. H. Kim, Y. J. Song, C. Kim, Y. Kim and S.-J. Kim, *Chem. – Eur. J.*, 2010, **16**, 4678; (*b*) R. V. Ottenbacher, K. P. Bryliakov and E. P. Talsi, *Inorg. Chem.*, 2010, **49**, 8620.

6 C. Zondervan, R. Hage and B. L. Feringa, *Chem. Commun.*, 1997, 419.

7 G. A. Barf and R. A. Sheldon, *Mol. Catal.*, 1995, **102**, 23.

8 R. A. Sheldon, *Chem. Commun.*, 2008, 3352.

9 (*a*) R. Noyori, M. Aoki and K. Sato, *Chem. Commun.*, 2003, 1977; (*b*) G. Grigoropoulou, J. H. Clark and J. A. Elings, *Green Chem.*, 2003, **5**, 1; (*c*) N. Mizuno, K. Yamaguchi and K. Kamata, 36th Int. Conf. Coord. Chem. Merida Mex., July 2004, 2005, 249, 1944.

10 Y. Sawada, K. Matsumoto and T. Katsuki, *Angew. Chem., Int. Ed.*, 2007, **46**, 4559.

11 A. U. Barlan, A. Basak and H. Yamamoto, *Angew. Chem., Int. Ed.*, 2006, **118**, 5981.

12 (*a*) D. C. Duncan, R. C. Chambers, E. Hecht and C. L. Hill, *J. Am. Chem. Soc.*, 1995, **117**, 681; (*b*) Y. Ishii, K. Yamawaki, T. Ura, H. Yamada, T. Yoshida and M. Ogawa, *J. Org. Chem.*, 1988, **53**, 3587; (*c*) M. Carraro, L. Sandei, A. Sartorel, G. Scorrano and M. Bonchio, *Org. Lett.*, 2006, **8**, 3671; (*d*) K. Kamata, M. Kotani, K. Yamaguchi, S. Hikichi and N. Mizuno, *Chem. – Eur. J.*, 2006, **13**, 639.

13 (*a*) C. Venturello, R. D'Aloisio, J. C. J. Bart and M. Ricci, *J. Mol. Catal.*, 1985, **32**, 107; (*b*) R. Neumann and M. Gara, *J. Am. Chem. Soc.*, 1995, **117**, 5066.

14 (*a*) N. Mizuno and K. Yamaguchi, *Chem. Rev.*, 2006, **6**, 12; (*b*) I. V. Kozhevnikov, *Catalysis by Polyoxometalate*, John Wiley & Sons, Chichester, UK, 2002; (*c*) K. Kamata, K. Yonehara, Y. Sumida, K. Yamaguchi, S. Hikichi and N. Mizuno, *Science*, 2003, **300**, 964; (*d*) B. Zhang, S. Li, A. Pöthig, M. Cokoja, S. L. Zang, W. A. Herrmann and F. E. Kühn, *Z. Naturforsch., B: J. Chem. Sci.*, 2013, **68b**, 587; (*e*) L. R. Graser, S. Jürgens, M. E. Wilhelm, M. Cokoja, W. A. Herrmann and F. E. Kühn, *Z. Naturforsch., B: J. Chem. Sci.*, 2013, **68b**, 1138.

15 (*a*) S. Omwoma, W. Chen, R. Tsunashima and Y.-F. Song, *Coord. Chem. Rev.*, 2014, **258**, 58; (*b*) S.-S. Wang and G.-Y. Yang, *Chem. Rev.*, 2015, **115**, 4893; (*c*) A. Proust, B. Matt, R. Villanneau, G. Guillemot, P. Gouzerh and G. Izzet, *Chem. Soc. Rev.*, 2012, **41**, 7605; (*d*) K. Kamata, K. Yonehara, Y. Nakagawa, K. Uehara and N. Mizuno, *Nat. Chem.*, 2010, **2**, 478; (*e*) S.-T. Zheng and G.-Y. Yang, *Chem. Soc. Rev.*, 2012, **41**, 7623; (*f*) P. Ma, R. Wan, Y. Si, F. Hu, Y. Wang, J. Niu and J. Wang, *Dalton Trans.*, 2015, **44**, 11514; (*g*) J. Lu, X. Zhang, P. Ma, V. Singh, C. Zhang, J. Niu and J. Wang, *J. Mater. Sci.*, 2018, **53**, 3078.

16 (*a*) P. Gouzerh and A. Proust, *Chem. Rev.*, 1998, **98**, 77; (*b*) A. R. Siedle, C. G. Markell, P. A. Lyon, K. O. Hodgson and A. L. Roe, *Inorg. Chem.*, 1987, **26**, 219; (*c*) D. K. Lyon and R. G. Finke, *Inorg. Chem.*, 1990, **29**, 1787; (*d*) N. Mizuno, D. K. Lyon and R. G. Finke, *J. Catal.*, 1991, **128**, 84; (*e*) N. Mizuno, H. Weiner and R. G. Finke, *J. Mol. Catal. A: Chem.*, 1996, **114**, 15; (*f*) Y. Imada, T. Shido, R. Ohnishi, K. Isobe and M. Ichikawa, *Catal. Lett.*, 1996, **38**, 101; (*g*) J. Lu, X. Ma, V. Singh, Y. Zhang, P. Ma, C. Zhang, J. Niu and J. Wang, *Dalton Trans.*, 2018, **47**, 5279; (*h*) J. Jia, Y. Niu, P. Zhang, D. Zhang, P. Ma, C. Zhang, J. Niu and J. Wang, *Inorg. Chem.*, 2017, **56**, 10131; (*i*) J. Li, J. Guo, J. Jia, P. Ma, D. Zhang, J. Niu and J. Wang, *Dalton Trans.*, 2016, **45**, 6726.

17 M. Bösing, A. Nöh, I. Loose and B. Krebs, *J. Am. Chem. Soc.*, 1998, **120**, 7252.

18 E. M. Limanski, D. Drewes, E. Droste, R. Böhner and B. Krebs, *Stud. Supramol. Chem. Mol. Struct.*, 2003, **656**, 17.

19 U. Kortz, N. K. Al-Kassem, M. G. Savelieff, N. A. Al Kadi and M. Sadakane, *Inorg. Chem.*, 2001, **40**, 4742.

20 U. Kortz, M. G. Savelieff, B. S. Bassil, B. Keita and L. Nadjo, *Inorg. Chem.*, 2002, **41**, 783.

21 J. Gao, J. Yan, S. Beeg, D.-L. Long and L. Cronin, *Angew. Chem., Int. Ed.*, 2012, **51**, 3373–3376.

22 Y. Liu, Y. Zhang, P. Ma, Y. Dong, J. Niu and J. Wang, *Inorg. Chem. Commun.*, 2015, **56**, 45.

23 G. M. Sheldrick, *SADABS Bruker AXS area detector scaling and absorption, version 2008/2001*, University of Göttingen, Germany, 2008.

24 O. V. Dolomanov, L. J. Bourhis, R. J. Gildea, J. A. K. Howard and H. Puschmann, *J. Appl. Crystallogr.*, 2009, **42**, 339.

25 (*a*) G. M. Sheldrick, *Acta Crystallogr., Sect. A: Fundam. Crystallogr.*, 2008, **64**, 112; (*b*) G. M. Sheldrick, *Acta Crystallogr., Sect. C: Cryst. Struct. Commun.*, 2015, **71**, 3.

26 (*a*) M. Bösing, I. Loose, H. Pohlmann and B. Krebs, *Chem. – Eur. J.*, 2006, **3**, 1232; (*b*) I. Loose, E. Droste, M. Bösing, H. Pohlmann, M. H. Dickman, C. Rosu, M. T. Pope and B. Krebs, *Inorg. Chem.*, 1999, **38**, 2688.

27 C. Zhao, C. S. Kambara, Y. Yang, A. L. Kaledin, D. G. Musaev, T. Lian and C. L. Hill, *Inorg. Chem.*, 2013, **52**, 671.

28 L. Yang, X. Ma, P. Ma, J. Hua and J. Niu, *Cryst. Growth Des.*, 2013, **13**, 2982.

29 (*a*) R. Villanneau, R. Delmont, A. Proust and P. Gouzerh, *Chem. Weinh. Bergstr. Ger.*, 2000, **6**, 1184; (*b*) A. V. Besserguenev, M. H. Dickman and M. T. Pope, *Inorg. Chem.*, 2001, **40**, 2582; (*c*) R. Villanneau, A. Proust, F. Robert and P. Gouzerh, *Chem. – Eur. J.*, 2003, **9**, 1982.

30 P. Zhang, V. Singh, J. Jia, D. Zhang, P. Ma, J. Wang and J. Niu, *Dalton Trans.*, 2018, **47**, 9317.

31 (*a*) L. Bai, K. Li, Y. Yan, X. Jia, J.-M. Lee and Y. Yang, *ACS Sustainable Chem. Eng.*, 2016, **4**, 437; (*b*) Z. Asgharpour, F. Farzaneh and A. Abbasi, *RSC Adv.*, 2016, **6**, 95729.